Research Square

Preprints are preliminary reports that have not undergone peer review.
They should not be considered conclusive, used to inform clinical practice,
or referenced by the media as validated information.

Climatic Suitability Shifts for Date Palm (Phoenix dactylifera L.) in Iran Over Four Past Decades (1980-2019)

Zahra Hosseini
University of Tehran
Javad Bazrafshan
jbazr@ut.ac.ir
University of Tehran
Arezoo Nazi Ghameshlou
University of Tehran

Research Article

Keywords: Date Palm, MaxEnt, Habitat Suitability, Decadal Shifts, Bioclimatic Variables, Iran

Posted Date: August 31st, 2026

DOI: https://doi.org/10.21203/rs.3.rs-10638836/v1

License: This work is licensed under a Creative Commons Attribution 4.0 International License.
Read Full License

Additional Declarations: No competing interests reported.

Climatic Suitability Shifts for Date Palm (*Phoenix dactylifera* L.) in Iran Over Four Past Decades (1980-2019)

Zahra Hosseini[1], Javad Bazrafshan[2*], Arezoo Nazi Ghameshlou[2]

[1]MSc Student, Department of Irrigation and Reclamation Engineering, University of Tehran, Karaj, Iran.

[2]Associate Professor, Department of Irrigation and Reclamation Engineering, University of Tehran, Karaj, Iran.

[*] Corresponding author (jbazr@ut.ac.ir, Address: College of Agriculture & Natural Resources, University of Tehran, Daneshkadeh Ave., Karaj, Iran; Postal Code: 3158777871. Phone Number: +982632241119)

Abstract

Climate change threatens agricultural systems in arid regions, yet historical shifts in crop suitability remain poorly documented. This study presents the first retrospective, multi-decadal assessment of climatic suitability shifts for date palm in Iran over four decades (1980–2019). Using MaxEnt with presence-only data (n=104) and 22 environmental variables, we reconstructed decadal suitability maps, identified key climatic drivers, and quantified spatiotemporal changes. Model performance was robust across all decades (AUC>0.8). BIO1 (Annual Mean Temperature) was the dominant predictor (68.1% contribution), increasing from 60.6% to 75.6% over time. Unsuitable areas dominated (>80% of Iran's land), yet high suitability reached its maximum extent (19.8×10^4 km²) in the 2010s, while medium suitability contracted to its minimum (13.2×10^4 km²), suggesting habitat polarization. Spatiotemporal analysis revealed a consistent west-to-east redistribution of suitable habitats, with decreased suitability in western provinces (Khuzestan, Fars) and increased suitability in southeastern regions (Kerman, Sistan and Baluchestan). The largest net increase in suitability (1.52%) occurred in the 2010s relative to the 1980s, while the most recent decade exhibited the smallest changes, suggesting potential stabilization. These findings provide critical benchmarks for validating future projections and informing adaptation strategies, including orchard relocation and cultivar selection.

Keywords: Date Palm, MaxEnt, Habitat Suitability, Decadal Shifts, Bioclimatic Variables, Iran.

1. Introduction

Climate change represents the most formidable challenge of the twenty-first century, threatening global food security through multiple pathways, including reduced agricultural productivity (Hultgren et al., 2025; Anshida et al., 2026). Climatic conditions, primarily through temperature regimes and water availability, fundamentally influence plant growth and development processes, thereby altering the geographic distribution and yield of agricultural crops at global scales (Challinor et al., 2015; Proctor et al., 2025). Global warming has induced poleward shifts of temperate zones (Chen et al., 2011; Heikonen et al., 2025), while the unprecedented increase in extreme climatic events—including heatwaves, droughts, and floods—has substantially reduced potential crop yields in areas with marginal climatic suitability (Fahad et al., 2017; Tuninetti and Davis, 2026). Consequently, identifying climatically suitable zones and monitoring their spatiotemporal dynamics in response to climate change has emerged as a strategic priority for climate adaptation planning (Dawson et al., 2011; Guisan et al., 2013).

The date palm (*Phoenix dactylifera* L.) is a cornerstone of agriculture in arid and semi-arid regions, providing food security and economic value across the Middle East and North Africa (Chao and Krueger, 2007; Shabani et al., 2012). This perennial crop has evolved remarkable adaptation to dry and semi-dry climatic conditions, requiring long, hot summers devoid of rainfall (Morton, 1987). Optimal vegetative growth occurs between 30 and 35°C (Zaid and *de* Wet, 2002), while flowering and fruit maturation demand sustained high temperatures, low relative humidity, and virtually no rainfall (Ismail et al., 2023). Cool winter temperatures below approximately −7°C can cause lethal damage (Morton, 1987; Zaid and de Wet, 2002), and high atmospheric humidity during the ripening period promotes fungal diseases and compromises fruit quality (Shabani et al., 2012; Hussain et al., 2020). Iran, as one of the world's leading date producers and a primary center of genetic diversity for this crop, cultivates date palm predominantly in its southern provinces, where climatic conditions have historically met these narrow ecological requirements. Beyond its economic value, date palm orchards provide critical ecosystem services in arid regions, including soil erosion reduction and desertification control (Mihi et al., 2019).

Despite the historical adaptation of date palm to Iran's warm climate, ongoing global warming and shifting precipitation patterns pose serious threats to this vital crop. One of the most alarming manifestations of this threat is the *bunch drying* disorder, which has recently caused annual losses of approximately 20–25% of total date production in Iran. Field investigations have demonstrated that the simultaneous occurrence of temperatures exceeding 43°C, relative humidity below 20%, and strong summer winds plays a critical role in triggering this physiological disorder (Najafiniya and Rahkhodaei, 2024). Given projections of increased frequency of such climatic extremes in Iran, especially in its southern parts (Bazrafshan, 2017; Jahanshahi et al., 2024; Asadi-RahimBeygi et al., 2025), incorporating

extreme temperature and humidity variables alongside mean climatic parameters in date palm suitability modeling has become an urgent necessity.

Species distribution models (SDMs) are widely employed to quantify climate–species relationships and to map habitat suitability under past, present, and future conditions (Elith et al., 2011; Phillips et al., 2017). Among the available algorithms, the maximum entropy approach implemented in MaxEnt is especially suitable for presence-only data and consistently yields robust predictions for crop species (Phillips et al., 2006; Ramirez-Cabral et al., 2017). MaxEnt offers the unique advantage of functioning effectively with presence-only occurrence records and demonstrates high performance when confronted with limited data (Elith et al., 2011; Yackulic et al., 2013). Furthermore, the use of bioclimatic variables (BCVs) rather than raw meteorological data has become a standard approach in this field, owing to their capacity to capture seasonal trends, annual fluctuations, and extreme events (Merkenschlager et al., 2023). MaxEnt models can be driven by high-resolution gridded climate surfaces, such as those provided by WorldClim, which offer historical monthly normals and derived bioclimatic variables at different spatial resolutions (Fick and Hijmans, 2017; Karger et al., 2017). The availability of historical time-slice data from WorldClim enables the reconstruction of decadal climate conditions, thereby allowing SDMs to be applied in a true retrospective framework that tracks suitability changes over time (Booth et al., 2014; Watling et al., 2021).

Previous studies have extensively projected future climate suitability for date palm. Global-scale research (e.g., Allbed et al., 2017 in Saudi Arabia) indicates substantial contractions of suitable zones and poleward shifts under various climate change scenarios. At the national level in Iran, Shabani et al. (2014) employed the CLIMEX model, while Baaghideh et al. (2020) utilized three GCMs to project the relative expansion of warm suitable zones in central Iran by 2080. Additionally, Afzali et al. (2022) applied MaxEnt to assess the future suitability of different date palm varieties. However, a comprehensive review of the literature reveals that all previous investigations have focused on future projections, with no study to date having objectively monitored the historical decadal shifts in date palm climatic boundaries based on observed bioclimatic data. This retrospective gap limits our ability to distinguish whether observed productivity declines are attributable to long-term climatic trends or short-term variability, and prevents the validation of future projections against already occurring changes (Dobrowski et al., 2011; Booth, 2018). While retrospective multi-decadal analyses that explicitly quantify suitability trajectories over recent historical decades are routine for wild species (Lenoir et al., 2008; Chen et al., 2011), they have rarely been applied to perennial fruit crops.

WorldClim's historical climate surfaces, now spanning multiple decades with improved accuracy, provide a unique opportunity to fill this gap by enabling the development of consistent, decadal-scale suitability maps for the recent past (Fick and Hijmans, 2017; Karger et al., 2017). Applying a MaxEnt-WorldClim framework to four consecutive decades in Iran would thus reveal not only the magnitude

of suitability shifts but also their rate and spatial pattern, offering directly translatable information for adaptation planning in one of the world's most climate-vulnerable date-producing regions (Shabani et al., 2013).

The primary objective of this study is to model the dynamic influence of climatic factors on date palm distribution and quantify shifts in optimal climatic boundaries across Iran over four decades (1980–2019). Using MaxEnt with presence-only occurrence data and environmental factors, we aim to: (1) reconstruct decadal suitability maps; (2) identify key environmental drivers and their response curves; and (3) quantify spatiotemporal changes in suitability classes.

2. Materials and Methods

2.1 Study area

Iran is located in Southwest Asia between approximately 25° N and 40° N latitude and 44° E to 64° E longitude, covering an area of around 1.65 million km². The country's climate is predominantly arid and semi-arid, exhibiting high spatial and temporal variability in temperature and precipitation (Khalili and Rahimi, 2018). Mean annual precipitation exceeds 1200 mm along the narrow Caspian Sea coast but drops below 100 mm in the central deserts and parts of the southeast (Modarres & Sarhadi, 2009). In contrast, summer maximum temperatures regularly surpass 50 °C in the interior lowlands, while winter minima can fall below −20 °C in the mountainous northwest (Alizadeh-Choobari & Najafi, 2018). Observational records show that Iran has experienced a marked warming trend over recent decades, with mean annual temperature increasing at rates well above the global average (Tabari & Talaee, 2011; Bazrafshan et al., 2017; Jamali et al., 2026).

Iran ranks third globally in date production (after Egypt and Saudi Arabia), with an average harvested area of 177,000 ha of productive date palm orchards and an average annual production of one million tons of various date cultivars over the period 1994–2024 (FAO, 2026). The provinces of Kerman, Hormozgan, Khuzestan, Bushehr, Fars, and Sistan and Baluchestan collectively account for more than 98% of the country's total date production, making them the major date-producing regions. Analysis of FAO (2026) data reveals that the harvested date area increased from 150,000 ha in 1994 to a peak of over 220,000 ha in 2011, followed by a declining trend that brought it down to 135,000 ha by 2024. This declining trend in the 2010s is similarly reflected in total date productions.

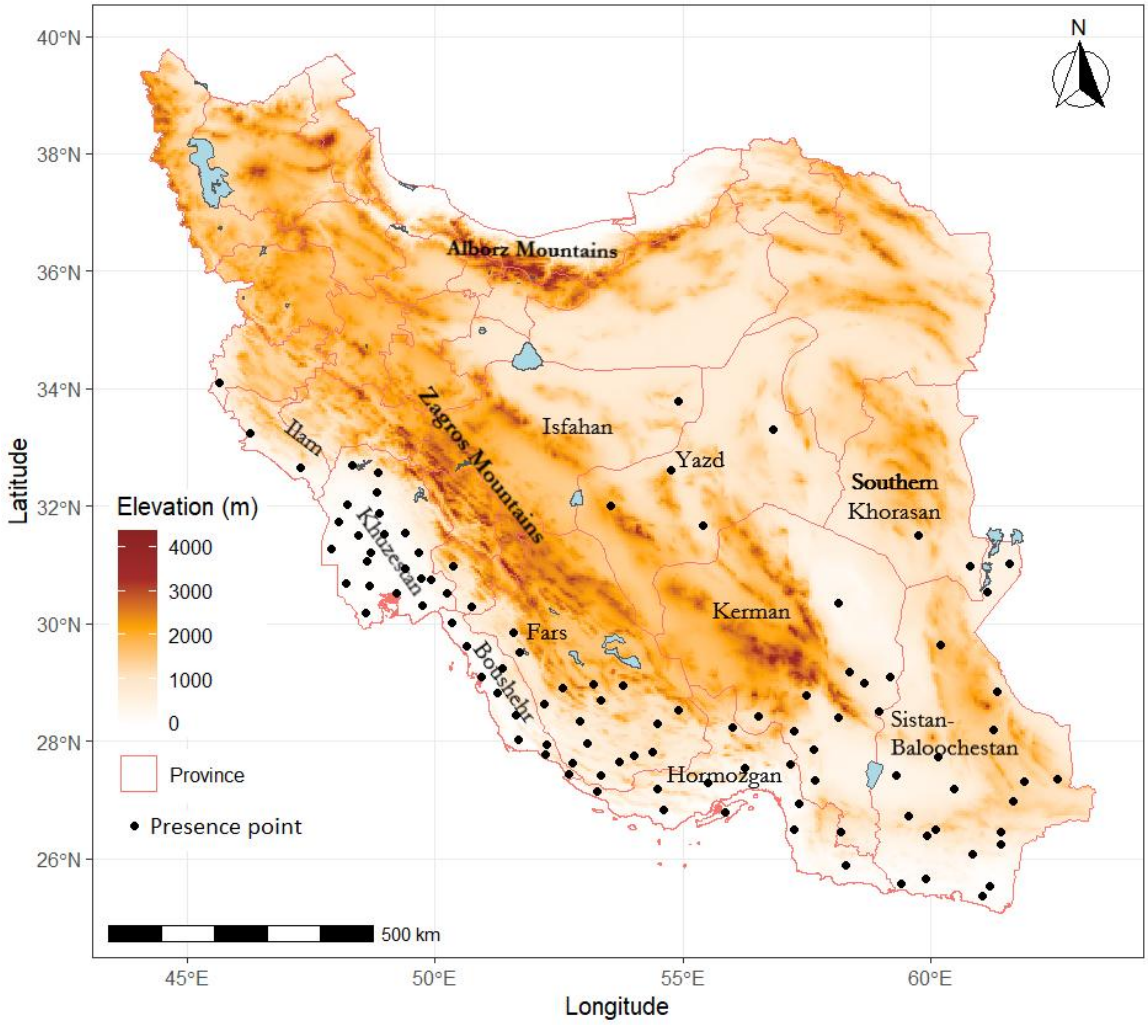


Fig. 1. Spatial distribution of date palm (*Phoenix dactylifera* L.) occurrence points in Iran (Source: Iran's Ministry of Agriculture, Unpublished document).

2.2 Species Occurrence Data

Occurrence data for date palm (n=104) were extracted from the archive of Iran's Ministry of Agriculture. The spatial locations of date palm presence in Iran (regardless of cultivar) are shown in Fig. 1. As illustrated in this figure, date palms are predominantly cultivated in six southern provinces of Iran, namely Kerman, Hormozgan, Khuzestan, Bushehr, Fars, and Sistan and Baluchestan.

2.3 Environmental Variables

The environmental predictors employed in this study comprised two categories: bioclimatic and topographic variables. Bioclimatic variables were obtained from the WorldClim version 2.1 database

(Fick and Hijmans, 2017) [downloaded from https://www.worldclim.org] and consist of 19 climatic indices (BIO1–BIO19; Table 1) derived from monthly temperature and precipitation data. These variables capture key ecological dimensions, including temperature and precipitation seasonality as well as extreme climatic conditions, and are consequently well-suited for species distribution modeling. All 19 bioclimatic variables were acquired at 2.5 arc-minute spatial resolution (~ 4 km) for four consecutive 10-year periods spanning 1980–2019. Topographic variables—specifically elevation, slope, and aspect—were derived from a digital elevation model with the 2.5 arc-minute resolution. These topographic predictors were used in conjunction with the bioclimatic variables as potential inputs for modeling date palm distribution across Iran.

Table 1. Input variables used in the MaxEnt model.

Variable	Description	Variable	Description
BIO1	Annual Mean Temperature (°C)	**BIO12**	Annual Precipitation (mm)
BIO2	Mean Diurnal Range (°C)	**BIO13**	Precipitation of Wettest Month (mm)
BIO3	Isothermality (BIO2/BIO7 ×100) (%)	**BIO14**	Precipitation of Driest Month (mm)
BIO4	Temperature Seasonality (SD ×100) (°C)	**BIO15**	Precipitation Seasonality (CV) (%)
BIO5	Max Temperature of Warmest Month (°C)	**BIO16**	Precipitation of Wettest Quarter (mm)
BIO6	Min Temperature of Coldest Month (°C)	**BIO17**	Precipitation of Driest Quarter (mm)
BIO7	Temperature Annual Range (BIO5–BIO6) (°C)	**BIO18**	Precipitation of Warmest Quarter (mm)
BIO8	Mean Temperature of Wettest Quarter (°C)	**BIO19**	Precipitation of Coldest Quarter (mm)
BIO9	Mean Temperature of Driest Quarter (°C)	**SLOPE**	Slope (%)
BIO10	Mean Temperature of Warmest Quarter (°C)	**ASPECT**	Aspect (°)
BIO11	Mean Temperature of Coldest Quarter (°C)	**ELEVATION**	Elevation (meters above sea level)

2.4 Mathematical Structure of the MaxEnt Model

The MaxEnt model is a machine learning method based on the principle of maximum entropy, specifically designed for modeling species distributions using presence-only data. In other words, we know the locations where the species has been observed, but definitive data on its absence are unavailable (Phillips et al., 2006). The fundamental principle of this approach is to estimate the most uniform (i.e., maximum entropy) probability distribution for the species across the study area, subject to known environmental constraints. The model is constructed such that the mean of each environmental variable in the estimated distribution matches the empirical mean of that variable at the species occurrence points (Phillips and Dudík, 2008).

2.4.1 Estimation of the Presence Probability Distribution

Assuming the study area consists of N equally sized grid cells (pixels), we define the vector $\pi = [\pi_1, \pi_2, \dots, \pi_N]$ as the true probability distribution of random species presence in each cell, and the vector $Q = [q_1, q_2, \dots, q_N]$ as the probability distribution estimated by the MaxEnt model. Let Z denote the $N \times s$ matrix of environmental predictors, where s is the number of predictor variables. The MaxEnt algorithm seeks the distribution Q that maximizes the entropy $H(Q)$:

$$H(Q) = -\sum_{i=1}^{N} q_i \ln(q_i) \quad (1)$$

subject to two constraints (Merow et al., 2013). First, the normalization constraint ensures that the estimated probabilities sum to unity:

$$\sum_{i=1}^{N} q_i = 1 \quad (2)$$

Second, for each feature function f_j (Sub-section 2.4.2), the expected value under the estimated distribution must equal the empirical average calculated from the presence records:

$$\sum_{i=1}^{N} q_i f_j(Z_i) = \frac{1}{n} \sum_{k=1}^{n} f_j(Z_k) = \bar{f}_j \quad (3)$$

where n is the number of presence points, Z_k is the vector of environmental variables at the k-th presence location, and $\bar{f}_j$ denotes the empirical mean of feature f_j. The left-hand side is computed across all grid cells, while the right-hand side is computed only at the presence points.

To solve this constrained optimization problem, the method of Lagrange multipliers is employed. By introducing Lagrange multipliers $\lambda_0, \lambda_1, \dots, \lambda_m$, the following function is maximized:

$$\mathcal{L} = -\sum_i q_i \ln q_i - \lambda_0 \left(\sum_i q_i - 1\right) - \sum_{j=1}^{m} \lambda_j \left(\sum_i q_i f_j(\boldsymbol{Z}_i) - \bar{f}_j\right) \quad (4)$$

By differentiating $\mathcal{L}$ with respect to q_i and setting the derivative to zero, the explicit form of the MaxEnt distribution is obtained (Phillips and Dudík, 2008):

$$q_i = \frac{\exp\left(\sum_{j=1}^{m} \lambda_j f_j(\boldsymbol{Z}_i)\right)}{\sum_{k=1}^{N} \exp\left(\sum_{j=1}^{m} \lambda_j f_j(\boldsymbol{Z}_k)\right)} = \frac{\exp(\eta(Z))}{Z(\lambda)} = q(Z) \quad (5)$$

This equation is essentially a distribution from the exponential family (specifically, a Gibbs distribution). In Eq. (5), i indexes a specific grid cell, j indexes the environmental variables, and k indexes the grid cells in the denominator. The term $Z(\lambda)$ is the normalization constant (partition function) that ensures the sum of probabilities equals unity, and $\eta(Z)$ is the linear predictor, representing the weighted sum of the environmental features.

2.4.2 Feature Functions

The MaxEnt model permits the use of multiple feature types—linear, quadratic, product, threshold, and categorical—to capture complex and nonlinear relationships between environmental predictors

and species distributions (Phillips and Dudík, 2008). The available feature types and their mathematical forms are summarized in Table 2.

Table 2. Feature types used in the MaxEnt model.

Feature Type	Mathematical Form	Equation Components
Linear	$f(x) = \lambda \cdot \frac{(x-k_1)}{(k_2-k_1)}$	x: environmental variable value at a given grid cell; k_1: lower bound of the environmental variable; k_2: upper bound of the environmental variable; λ: Lagrange multiplier for the environmental variable
Quadratic	$f(x) = \lambda \cdot \frac{(x^2-k_1)}{(k_2-k_1)}$	
Product	Product of two variables	Two environmental variables multiplied together
Threshold	Binary transformation (0 or 1)	Variable converted to presence/absence based on a threshold value
Categorical	Features for categorical variables	Qualitative variables

2.4.3 Regularization

To mitigate overfitting, MaxEnt incorporates a regularization parameter, which modifies the objective function as follows (Merow et al., 2013):

$$\text{Maximize } H(\boldsymbol{Q}) - \sum_j \beta_j \left|\lambda_j\right| \quad (6)$$

where β_j is the regularization coefficient for feature j. This formulation is equivalent to maximizing the log-likelihood with an ℓ_1 (LASSO) penalty (Warren and Seifert, 2011). Regularization serves three critical functions: (1) it drives the weights of irrelevant features to exactly zero, effectively removing noise; (2) it prevents the coefficients λ_j from becoming excessively large, ensuring numerical stability; and (3) it produces a smoothed probability distribution that generalizes to new data rather than overfitting to the training occurrences (Dudik et al., 2007).

2.4.4 Calculating Species Presence Probability

In MaxEnt modeling for species, q_i represents the relative probability density of selecting the i-th grid cell, rather than the absolute probability of species presence. To convert this relative density into the conditional presence probability $P(y = 1|\boldsymbol{Z})$, we apply Bayes' rule. We assume that presence points ($y = 1$) follow the MaxEnt distribution $q(\boldsymbol{Z})$, while absence points ($y = 0$) are sampled uniformly from the entire landscape, i.e., $P(\boldsymbol{Z}|y = 0) = \frac{1}{N}$, where N is the number of grid cells.

According to Bayes' rule:

$$P(y = 1|\boldsymbol{Z}) = \frac{P(\boldsymbol{Z}|y=1)\cdot P(y=1)}{P(\boldsymbol{Z}|y=1)\cdot P(y=1)+P(\boldsymbol{Z}|y=0)\cdot P(y=0)} \quad (7)$$

Let M be the number of presence records and $r = \frac{P(y=1)}{P(y=0)} = \frac{M/\mathrm{N}}{1-M/\mathrm{N}} \approx \frac{M}{N}$ be the prior odds. Substituting $P(\boldsymbol{Z}|y=1) \propto q(\boldsymbol{Z}) = \frac{\exp(\eta(\boldsymbol{Z}))}{\boldsymbol{Z}(\lambda)}$ yields:

$$P(y=1|\boldsymbol{Z}) = \frac{1}{1+\frac{(1-r)\cdot \boldsymbol{Z}(\lambda)}{r\cdot N}\cdot \exp(-\eta(\boldsymbol{Z}))} \quad (8)$$

The output of this logistic transformation ranges from 0 to 1 and is interpreted as the probability of species presence in the grid cell. This formulation is commonly referred to as the logistic output in MaxEnt software and is widely preferred over the raw output for its interpretability and direct ecological relevance (Phillips and Dudík, 2008; Merow et al., 2013).

2.5 Multicollinearity Analysis and Variable Selection

To mitigate multicollinearity among environmental predictors, which can compromise model stability and variable interpretation, a Pearson correlation analysis was performed on all 22 candidate variables. Variable pairs with a correlation coefficient exceeding $|\mathrm{r}| > 0.95$ were considered highly correlated (Feng et al., 2019). For each such pair, the variable with lower ecological relevance to date palm biology was excluded. Following this screening, five bioclimatic variables—BIO6 (Min Temperature of Coldest Month), BIO10 (Mean Temperature of Warmest Quarter), BIO11 (Mean Temperature of Coldest Quarter), BIO16 (Precipitation of Wettest Quarter), and BIO17 (Precipitation of Driest Quarter)—were removed from the candidate set. The remaining 17 variables (14 bioclimatic and 3 topographic) were retained as final inputs. Subsequently, the jackknife test was employed to evaluate the relative contribution and importance of each retained variable in the final MaxEnt model (Shi et al., 2021).

2.6 Species Distribution Modeling and Model Validation

Following variable selection (Subsection 2.5), the final set of environmental predictors was used to build MaxEnt models for each of the four decades. Species distribution modeling was performed using MaxEnt version 3.4.2 (Phillips et al., 2017). The retained environmental variables were imported as raster layers alongside the species occurrence records, which were formatted as a CSV file containing species name, longitude, and latitude. The model parameters were configured as follows: (a) 70% of the presence data were randomly allocated for model training and the remaining 30% were used for model testing; (b) species response curves were generated to explore the relationship between occurrence probability and each environmental predictor; (c) to prevent model overfitting, the regularization multiplier was set to 1.5 through trial and error and repeated iterations; (d) all other parameters were retained at their default values, including a convergence threshold of 10^{-5}, a maximum of 500 iterations, and a maximum of 10,000 background points (grid cells); and (e) cross-validation was selected as the replicate run type, and the model was executed 10 times for each of the four decades (1980–1989, 1990–1999, 2000–2009, and 2010–2019) to account for stochastic variability and ensure

model stability. The final habitat suitability map for each decade was derived by averaging the outputs from the 10 replicate runs.

2.7 Evaluation of MaxEnt Model Performance

Model performance was evaluated using the area under the curve (AUC) of the receiver operating characteristic (ROC), a standard metric for assessing the predictive accuracy of binary classification models (Marzban, 2004). The ROC curve plots the true positive rate (TPR; sensitivity) against the false positive rate (FPR; 1 – specificity) across all possible probability thresholds. For each threshold, a confusion matrix (Table 3) was constructed, summarizing the frequency of actual presence/absence observations against model predictions, where positive and negative denote predicted presence and predicted absence, respectively. TPR and FPR were calculated as:

$$TPR = \frac{TP}{TP+FN} \quad (9)$$

$$FPR = \frac{FP}{FP+TN} \quad (10)$$

where TP = true positives, FN = false negatives, FP = false positives, and TN = true negatives. TPR (sensitivity) measures the proportion of actual presence points correctly predicted as present, while FPR measures the proportion of actual absence points incorrectly predicted as present. After generating the ROC curve, the AUC was computed as the integral under the curve. AUC values range from 0 to 1, with higher values indicating superior discriminatory ability. According to the classification scheme of Swets (1988), model performance was categorized as: fail (0.5–0.6), poor (0.6–0.7), fair (0.7–0.8), good (0.8–0.9), and excellent (0.9–1.0).

Table 3. Confusion matrix for evaluating MaxEnt model performance.

	Predicted Presence	**Predicted Absence**
Actual Presence	True Positive (TP)	False Negative (FN)
Actual Absence	False Positive (FP)	True Negative (TN)

Note: TP = correctly predicted presence; FN = presence incorrectly predicted as absence; FP = absence incorrectly predicted as presence; TN = correctly predicted absence.

2.8 Classification of Date Palm Habitat Suitability

To classify habitat suitability for date palm, we adopted the threshold-based approach proposed by Shi et al. (2021). Under this scheme, grid cells were categorized into four suitability classes based on predicted presence probability: unsuitable (<0.05), low suitability (0.05–0.33), medium suitability (0.33–0.66), and high suitability (>0.66). The area of each suitability class was computed for each decade by summing the cell areas of all grid cells belonging to each class, enabling quantification of habitat gain or loss over time.

2.9 Spatiotemporal Changes in Date Palm Habitat Suitability

To facilitate a more straightforward assessment of Spatiotemporal changes in habitat suitability across consecutive decades, we employed a modified binary classification for comparative purposes: areas with a presence probability below 0.33 were classified as sub-optimal, while areas with a probability equal to or exceeding 0.33 were classified as optimal. This binary classification enabled the overlay of suitability maps from different decades, allowing for the identification of areas where climatic suitability has deteriorated (reduced), improved (increased), or remained stable over time, as described in Shi et al. (2021) and Wang et al. (2025).

3. Results

3.1 Model Performance and Validation

The mean Area Under the Curve (AUC) values for the MaxEnt models ranged from 0.836 to 0.845 (Fig. 2), indicating strong discriminatory ability between suitable and unsuitable habitats. The highest AUC was observed in the 1980s (0.845 ± 0.04), while the lowest was in the 2010s (0.836 ± 0.05), suggesting consistent model reliability across time periods. According to the classification of Swets (1988), these values indicate good model performance, providing confidence in the subsequent analysis of variable importance and habitat suitability patterns. Given this robust performance, we next examined the relative contribution of individual environmental variables to date palm distribution.

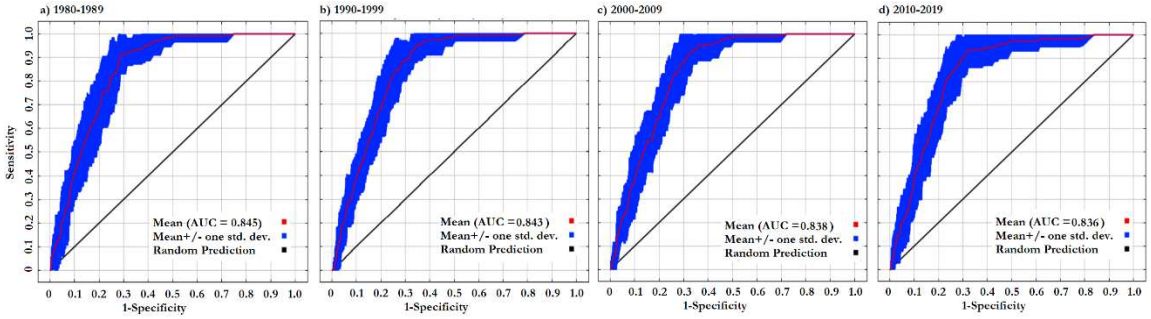


Fig. 2. Receiver operating characteristic (ROC) curves for the MaxEnt model test phase across the study periods: (a) 1980–1989, (b) 1990–1999, (c) 2000–2009, and (d) 2010–2019.

3.2 Variable Importance

3.2.1 Percent Contributions and Permutation Importance

The relative contributions of the 17 environmental predictors to the MaxEnt models were quantified using two metrics: percent contribution (PC), based on the regularized gain attributed to each variable during model fitting, and permutation importance (PI), which measures the decrease in AUC when the

variable's values are randomly permuted. Average values across the four decades, along with decadal trends, are summarized in Table 4.

BIO1 (Annual Mean Temperature) was the predominant predictor across all decades, with a mean PC of 68.1% and a mean PI of 56.3%. Its influence exhibited a clear increasing temporal trend: PC rose from 60.6% in the 1980s to 75.6% in the 2010s, while PI increased from 40.2% to 66.7% over the same period. Notably, PC consistently exceeded PI for BIO1 across all decades.

Among the remaining variables, BIO8 (Mean Temperature of the Wettest Quarter) and BIO19 (Precipitation of the Coldest Quarter) showed notable declining contributions. BIO8's PC decreased from 12.5% in the 1980s to 0.7% in the 2010s, while its PI declined from 9.4% to 4.1%. Similarly, BIO19 decreased from 6.2% (PC) and 7.6% (PI) in the earliest decade to 1.7% and 0.8%, respectively, in the most recent decade.

In contrast, the topographic predictors—ASPECT and ELEVATION—remained relatively stable across all decades. Their mean PC values were 3.5% and 2.4%, respectively, while their mean PI values were higher at 5.2% and 4.8%.

Table 4. Percent contribution (PC) and permutation importance (PI) of environmental variables in MaxEnt models for date palm distribution across four decades (1980s–2010s).

Environmental variable	1980s		1990s		2000s		2010s		Average	
	PC (%)	PI (%)	PC (%)	PI (%)	PC (%)	PI (%)	PC (%)	PI (%)	PC (%)	PI (%)
BIO1*	**60.6**	**40.2**	**68.1**	**63.8**	**67.9**	**54.5**	**75.6**	**66.7**	**68.1**	**56.3**
BIO2	0.3	0.4	0.5	0.5	0.5	1.1	0.5	1.6	0.5	0.9
BIO3	1.3	0.3	1.1	0.1	1.1	0.1	1.1	1.9	1.2	0.6
BIO4	1.1	**7.8**	0.8	1.7	1.8	**4.5**	1.0	0.3	1.2	3.6
BIO5	**3.4**	3.6	2.0	0.8	**3.0**	**9.1**	**3.3**	**3.9**	2.9	4.4
BIO7	0.5	0.0	0.6	0.6	0.8	2.6	1.0	3.9	0.7	1.8
BIO8*	**12.5**	**9.4**	**3.7**	**3.7**	**3.5**	2.3	0.7	**4.1**	**5.1**	**4.9**
BIO9	1.2	0.4	1.1	1.6	1.3	0.2	1.2	0.4	1.2	0.7
BIO12	1.0	**9.5**	1.4	**4.7**	0.6	0.9	0.3	0.4	0.8	3.9
BIO13	0.7	4.5	0.6	0.5	2.3	0.4	**3.5**	1.3	1.8	1.7
BIO14	0.3	2.1	0.1	1.7	0.0	0.8	0.1	1.0	0.1	1.4
BIO15	2.4	0.3	**2.7**	0.4	**6.1**	**5.9**	1.4	1.0	**3.2**	1.9
BIO18	0.9	1.2	0.8	0.5	2.2	3.3	1.1	1.5	1.3	1.6
BIO19*	**6.2**	**7.6**	**9.4**	**9.9**	2.0	3.1	1.7	0.8	**4.8**	**5.4**
ASPECT*	**3.6**	6.0	**3.4**	**4.8**	**3.3**	**5.6**	**3.6**	**4.5**	**3.5**	**5.2**
SLOPE	1.3	1.1	1.0	1.1	1.4	1.1	1.5	1.0	1.3	1.1
ELEVATION*	2.7	5.4	2.5	3.7	2.1	4.2	**2.4**	**5.8**	2.4	**4.8**

Note: Asterisks (*) indicate variables retained for the final MaxEnt model. Bold values represent the highest PC and PI for each decade.

BIO5 (Max Temperature of Warmest Month) and BIO12 (Annual Precipitation) showed moderate but sporadic importance, particularly BIO5 with a mean PI of 4.4% and a peak PC of 9.1% during the 2000s. The remaining variables, including those related to temperature seasonality (BIO4, BIO7) and precipitation seasonality (BIO15), contributed negligibly to the models, with mean PC values below 3.2%. The discrepancy between PC and PI for certain variables (e.g., BIO12) suggests

that while these variables contribute to model fitting, they may be correlated with other predictors and do not provide unique information when permuted.

Based on the combined evaluation of PC, PI, and temporal consistency across the four decades, five variables were suggested for the final MaxEnt model (Table 4; indicated by asterisks): BIO1, BIO8, BIO19, ASPECT, and ELEVATION.

3.2.2 Jackknife Test Results

The jackknife test results across four decades (1980s–2010s) have been represented in Fig. 3. The test evaluated the gain in model performance when each variable was used in isolation and the drop in gain when excluded. The MaxEnt output includes three jackknife formats: (1) regularized training gain, (2) test gain, and (3) AUC for test data, which measures the reduction in mean AUC when each variable is excluded. Higher gain values indicate greater model accuracy.

In the regularized training phase (Fig. 3, *upper panels*), for all four decades, BIO1 and BIO8 used in isolation produced high accuracy, while BIO14 and BIO2 yielded negligible gain. Excluding ASPECT caused the greatest accuracy reduction.

For the test phase (Fig. 3, *middle panels*), similar to the training phase, BIO1 and BIO8, when used in isolation, produced the highest accuracy across all four decades. However, the variable causing the greatest reduction in model performance varied by decade: BIO8 in the 1980s, BIO19 in the 1990s, BIO5 in the 2000s, and BIO7 in the 2010s. Notably, excluding SLOPE consistently improved model performance across all decades.

According to the AUC-based jackknife (Fig. 3, *lower panels*), BIO1, BIO8, and ELEVATION each achieved >75% accuracy when used alone. BIO14 showed minimal gaining across all four decades. No single variable exclusion substantially affected model accuracy.

These jackknife results further validate the variable selection procedure described in Subsection 3.2.1, confirming the retention of BIO1, BIO8, and ELEVATION as the most ecologically relevant predictors. Two other variables, ASPECT and BIO19, did not provide sufficient predictive power to enhance model accuracy, suggesting their limited independent contribution to date palm distribution modeling.

3.3 Response Curves

Response curves illustrate how each environmental variable influences MaxEnt predictions, showing the change in predicted presence probability as a given variable varies while all other variables are held at their mean values. As noted in the AUC-based jackknife results (Subsection 3.2.2), BIO1 (Annual Mean Temperature), BIO8 (Mean Temperature of the Wettest Quarter), and ELEVATION, when used in isolation, demonstrated high capability in discriminating presence from absence locations. Fig.

4 presents the response curves for these three variables for the earliest (1980s) and latest (2010s) decades.

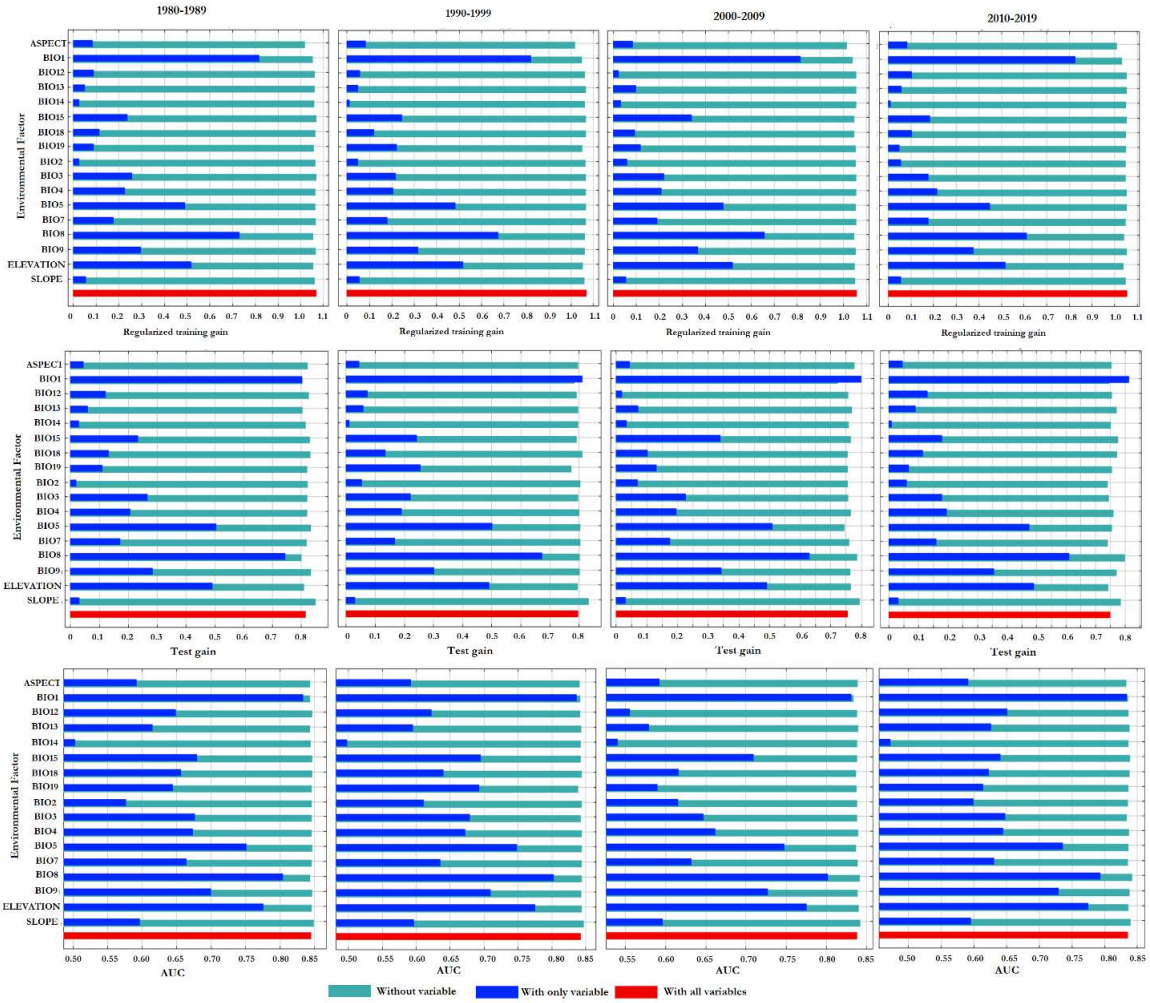


Fig. 3. Jackknife test results for MaxEnt models across four decades (1980s–2019s). The three rows show: (*upper*) training gain, (*middle*) test gain, and (*lower*) AUC for test data. Blue bars: gain when variable used alone; green bars: gain when variable excluded; red bars: gain using all variables.

For BIO1 (Fig. 4a, 1980s; Fig. 4b, 2010s), the highest presence probability (>80%) in the 1980s occurred when values ranged between 24°C and 27°C, with the maximum probability at 26.5°C. By the 2010s, the optimal temperature shifted upward by approximately 1°C, indicating a detectable shift in the species' thermal optimum as captured by the MaxEnt model. Furthermore, the standard deviation of the BIO1 response increased considerably from the 1980s to the 2010s, suggesting greater uncertainty in model predictions for the most recent decade.

The response curves for BIO8 (Mean Temperature of the Wettest Quarter) also exhibited temporal changes, with an increase in the standard deviation of the response and a shift in the breakpoint from 12.5°C in the 1980s to 15.5°C in the 2010s (Fig. 4c–d).

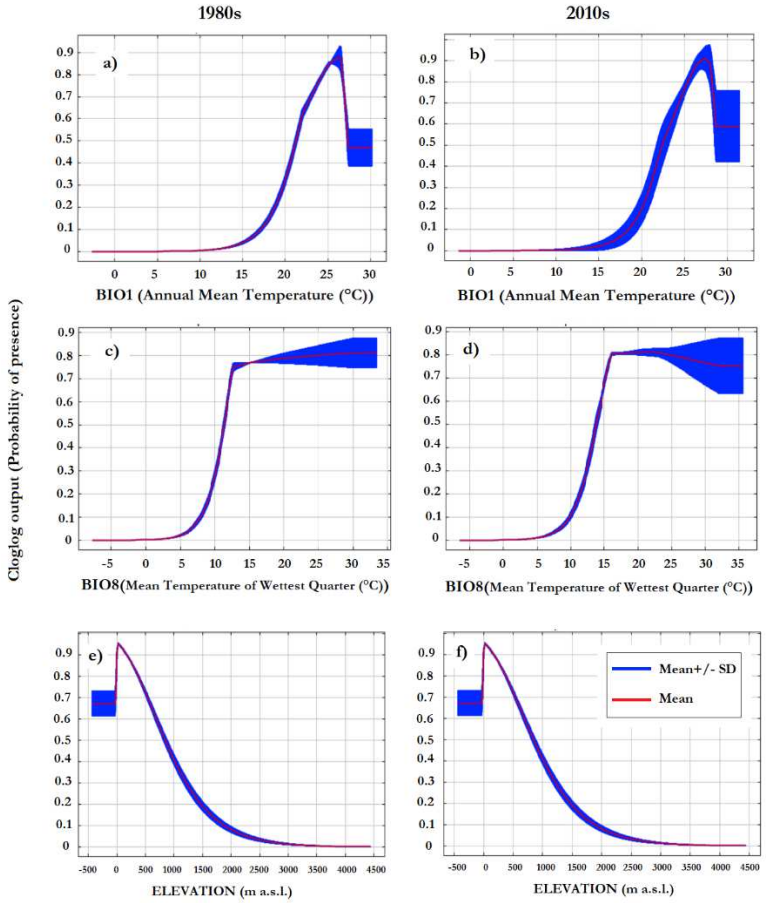


Fig. 4. Response curves for the three most influential variables—BIO1 (Annual Mean Temperature), BIO8 (Mean Temperature of the Wettest Quarter), and ELEVATION—for the (a, c, e) 1980s and (b, d, f) 2010s. Red lines indicate the mean response across 10 model replicates, and blue shaded areas represent ± one standard deviation.

In contrast, the response curves for ELEVATION showed little change over time (Fig. 4e–f). Presence probability remained high in low-elevation areas (<500 m a.s.l.) and declined rapidly with increasing elevation. Notably, the uncertainty associated with ELEVATION estimates remained low across both decades, enhancing its reliability for decision-making.

3.4 Spatial Patterns of Habitat Suitability

The spatial distribution of climatic suitability for date palm across Iran was mapped for each of the four decades (1980s–2010s) using the MaxEnt model outputs (Fig. 5a–d). Based on the classification scheme of Shi et al. (2021), grid cells were categorized into four suitability classes: unsuitable, low

suitable, medium suitable, and high suitable. The areal extent of each class, calculated by summing the areas of all grid cells belonging to each category, is summarized in Table 5.

The results indicate that unsuitable areas consistently dominated the landscape across all four decades, accounting for more than 80% of Iran's total land area (Table 5). This pattern reflects the predominantly arid and hyper-arid climatic conditions that prevail across much of the country, limiting date palm cultivation to specific environmentally favorable regions.

Suitable habitats (the sum of low, medium, and high suitable classes) covered approximately 77.2 $\times 10^4$ km² in the 1980s, representing 41.9% of the study area. However, a marked decline in overall suitable area occurred in the 1990s, falling to 70.4 $\times 10^4$ km² (39.5%), driven primarily by a reduction in medium and high suitability classes. Specifically, medium suitable areas decreased from 19.8 $\times 10^4$ km² in the 1980s to 15.5 $\times 10^4$ km² in the 1990s, while high suitable areas declined from 17.3 $\times 10^4$ km² to 14.8 $\times 10^4$ km².

In the 2000s, the total suitable area partially recovered to 77.5 $\times 10^4$ km² (41.9%), with notable increases in low suitability (44.2 $\times 10^4$ km²) and medium suitability (16.5 $\times 10^4$ km²). High suitability, however, remained lower (16.8 $\times 10^4$ km²) than in the 1980s. The most recent decade (2010s) exhibited a contrasting pattern: the low suitable class expanded to its maximum extent (44.7 $\times 10^4$ km²), while medium suitable areas contracted to their minimum (13.2 $\times 10^4$ km²). Conversely, the high suitable class reached its peak area (19.8 $\times 10^4$ km²), exceeding all previous decades.

The spatial distribution of high suitable areas showed a clear concentration in the southern provinces (Fig. 5a–d), including Kerman, Hormozgan, Khuzestan, Bushehr, Fars, and Sistan and Baluchestan, consistent with the current distribution of date palm orchards in Iran. High suitability was predominantly located in low-elevation areas with warm temperatures and limited precipitation, whereas unsuitable areas corresponded to the central deserts, northern cold regions, and high mountain ranges.

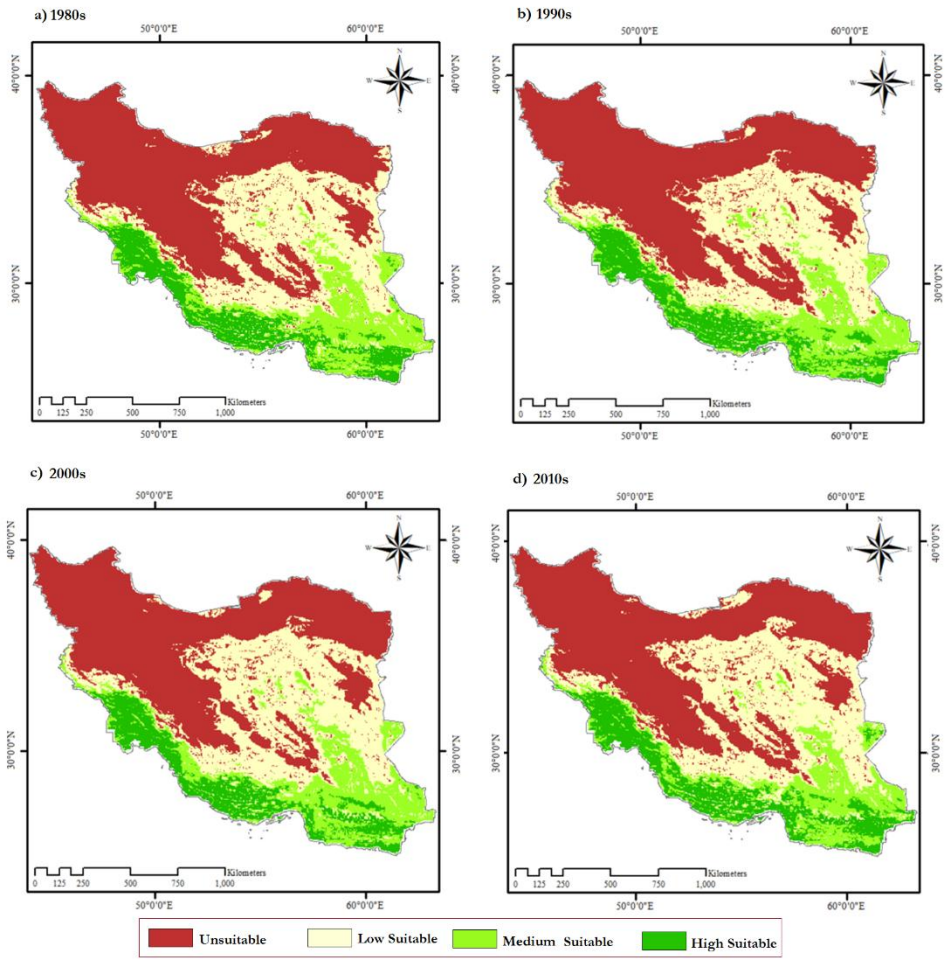


Fig. 5. Spatial distribution of climatic suitability for date palm in Iran across four decades (1980s–2010s).

Table 5. Areal extent ($\times 10^4$ km^2) of different climatic suitability classes for date palm in Iran across four consecutive decades.

Decade	Unsuitable ($\times 10^4$ km^2)	Low Suitable ($\times 10^4$ km^2)	Medium Suitable ($\times 10^4$ km^2)	High Suitable ($\times 10^4$ km^2)
1980s	87.4	40.1	19.8	17.3
1990s	94.4	40.1	15.5	14.8
2000s	87.0	44.2	16.5	16.8
2010s	87.7	44.7	13.2	19.8

3.5 Spatiotemporal Changes in Suitability Area

To better understand the spatial dynamics of date palm presence probability, as described in the subsection 2.8, the climatic suitability areas were reclassified into two binary categories, sub-optimal and optimal. The spatial distribution of these binary suitability classes was then overlaid across consecutive decades to examine shifts in climatic suitability of date palm distribution in response to

climatic changes. Areas with decreased suitability were defined as those that were classified as optimal class in a given decade but transitioned to sub-optimal class in the subsequent decade. Conversely, areas with increased suitability were those that were classified as sub-optimal class in a given decade but transitioned to optimal class in the following decade. Stable areas were those that maintained the same suitability classification across the study period.

Figure 6 presents the spatial patterns of changes in climatic suitability across different temporal comparisons. Panels (a) through (c) compare changes in climatic suitability in the 1990s, 2000s, and 2010s, respectively, relative to the baseline decade of the 1980s. Panels (d) and (e) assess changes in climatic suitability in the 2000s and 2010s, respectively, relative to the 1990s. Panel (f) evaluates changes in the 2010s relative to the 2000s. The areal extents of the changes shown in Fig. 6 are summarized in Table 6. The results reveal several important patterns, as follows.

3.5.1 Long-term changes relative to the 1980s baseline

As shown in Figure 6a, the 1990s experienced a notable loss of climatic suitability compared to the 1980s across several regions. Areas that lost suitability included parts of eastern Isfahan Province, western South Khorasan Province, northern Yazd Province, and multiple areas within Hormozgan, Fars, and Khuzestan provinces—regions that had previously been suitable for date palm cultivation. In contrast, improvements in climatic suitability were observed in portions of Sistan and Baluchestan, Kerman, and South Khorasan provinces, where the probability of date palm presence increased over the same period.

Compared to the 1980s, the 2000s (Fig. 6b) exhibited a more spatially heterogeneous pattern of change. The areas of decreased suitability, while reduced in extent compared to the 1990s, remained concentrated in the central and western provinces (e.g., Isfahan, Yazd, and parts of Fars). Areas of increased suitability were more widespread in the 2000s, with notable expansion in the southeastern provinces (Sistan and Baluchestan, Kerman) and limited gains in eastern regions (South Khorasan). Stable suitability areas formed a contiguous band across the central deserts and northern mountain ranges, reflecting regions where climatic conditions have remained consistently unfavorable for date palm cultivation.

The most pronounced long-term changes were observed in the 2010s compared to the 1980s (Fig. 6c). The area of increased suitability reached its maximum extent (1.52%), with gains distributed across a broader geographical range, including the eastern provinces, northern parts of Kerman, and scattered patches in the northwest. Conversely, the extent of decreased suitability was at its minimum (0.79%), primarily confined to the western and southwestern provinces (Khuzestan, Fars, and parts of Bushehr).

3.5.2 Sequential changes relative to the 1990s

The 2000s vs. 1990s comparison (Fig. 6d) revealed that the largest decrease (1.01%) occurred during this period, with losses concentrated in the central provinces (Isfahan, Yazd, and parts of Kerman) and the western provinces (Fars and Khuzestan). Gains were more limited (0.96%) and primarily observed in the eastern regions (South Khorasan, Sistan and Baluchestan). The dominant pattern during this period was one of relative stability, with approximately 74.49% of the landscape remaining unsuitable and 23.54% remaining stable.

The 2010s vs. 1990s comparison (Fig. 6e) showed a recovery in suitability gains, with increased suitability rising to 1.39% and decreased suitability declining to 0.96%. Spatial patterns of improvement were more pronounced in the southeastern provinces (Kerman, Sistan and Baluchestan) and eastern regions, while losses were primarily confined to the southwestern provinces (Khuzestan, Fars, and Bushehr), suggesting a regional redistribution of suitable areas from the west to the east and southeast.

3.5.3 Recent decadal changes

The 2010s vs. 2000s comparison (Fig. 6f) exhibited the most recent spatial patterns of change. Increased suitability (1.23%) and decreased suitability (0.74%) were both at their lowest levels, indicating a relatively stable period in terms of net change. Spatial patterns of increased suitability were concentrated in northern parts of Kerman, eastern provinces, and scattered patches along the northern fringes of the central deserts. Decreased suitability was limited to small, isolated patches in Khuzestan and Fars, with no large-scale contiguous losses. The stability of this period suggests that the climatic redistribution of suitable habitats may be approaching a new equilibrium following the more dynamic changes observed in previous decades.

Table 6. Areal extent (%) of changes in climatic suitability for date palm across different temporal comparisons in Iran.

Base Period	Subsequent Period	Unsuitable (%)	Increased (%)	Decreased (%)	Stable (%)
1980s	**1990s**	74.24	1.26	0.97	23.53
	2000s	74.36	1.09	0.85	23.70
	2010s	74.42	1.52	0.79	23.27
1990s	**2000s**	74.49	0.96	1.01	23.54
	2010s	74.54	1.39	0.96	23.11
2000s	**2010s**	74.71	1.23	0.74	23.33

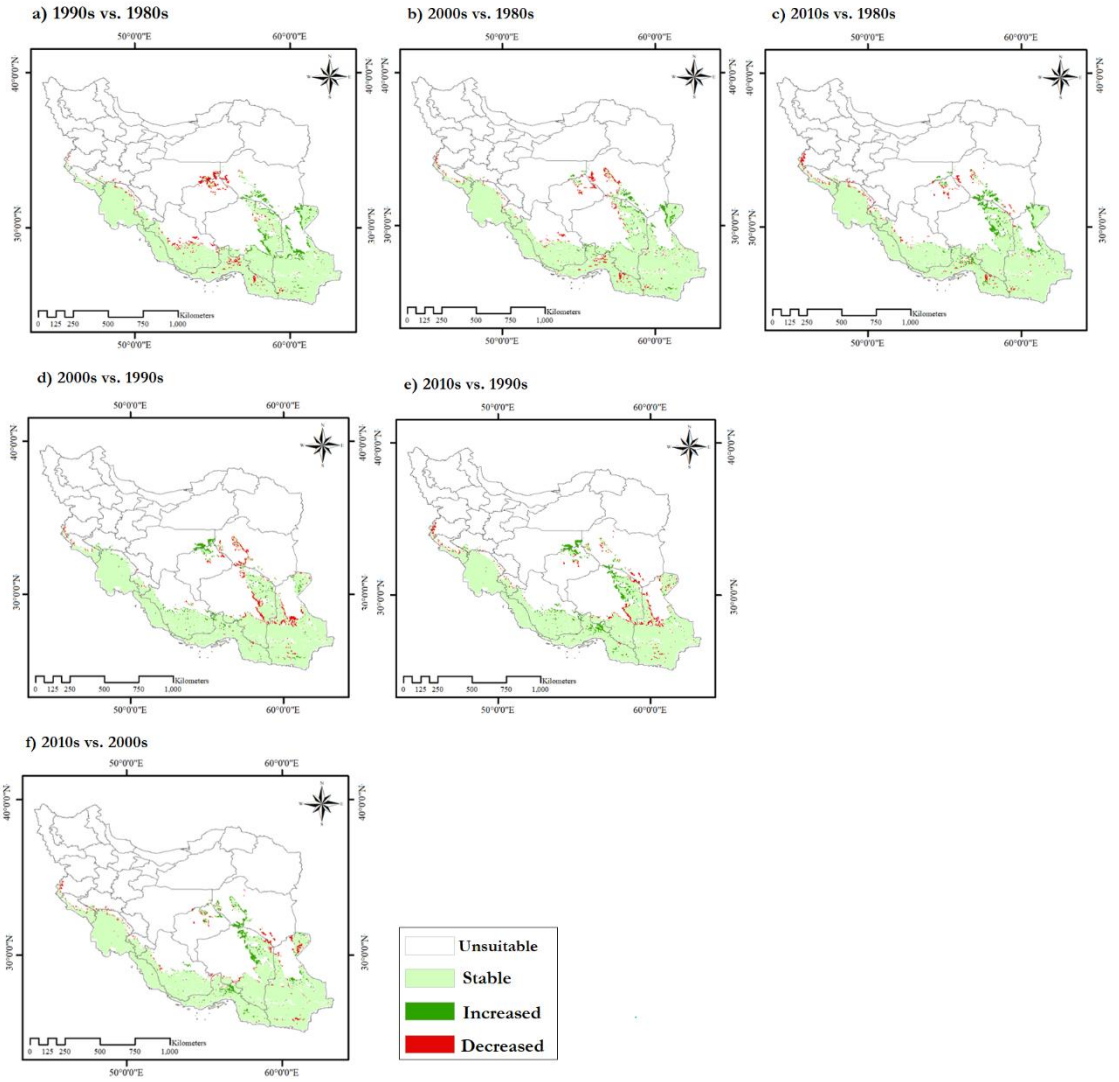


Fig. 6. Spatial patterns of changes in climatic suitability for date palm in Iran across different temporal comparisons: (a) 1990s vs. 1980s, (b) 2000s vs. 1980s, (c) 2010s vs. 1980s, (d) 2000s vs. 1990s, (e) 2010s vs. 1990s, and (f) 2010s vs. 2000s.

4. Discussion

The AUC values obtained in this study (0.836–0.845) indicate good model performance according to Swets (1988) classification, consistent with other MaxEnt studies on date palm. For instance, Mihi and Hernández-Agüero (2025) reported an AUC of 0.933 for date palm in Algeria, suggesting that regional differences in spatial scale, environmental predictors, and climatic variability may influence model performance. Shabani et al. (2017) compared multiple modeling techniques for date palm and found that MaxEnt provides comparable results to other correlative models, though model choice can affect projections. The slight temporal decline in AUC observed in our study—from 0.845 in the 1980s to

0.836 in the 2010s—may reflect increasing climatic variability and uncertainty in recent decades, consistent with broader regional warming trends documented across Iran (Tabari and Talaee, 2011; Bazrafshan, 2017).

Among all environmental predictors, BIO1 (Annual Mean Temperature) emerged as the overwhelmingly dominant variable, with a mean percent contribution of 68.1% across all decades, aligning with previous studies that identified temperature as the primary climatic constraint on date palm distribution (Shabani et al., 2012; Shabani and Kumar, 2014). The increasing contribution of BIO1 over time—from 60.6% in the 1980s to 75.6% in the 2010s—suggests that temperature has become an increasingly important determinant of suitable habitats as warming progresses. The response curves for BIO1 revealed an optimal temperature range of 24–27°C in the 1980s, shifting upward by approximately 1°C in the 2010s, indicating a detectable thermal adaptation response consistent with climate-driven range shifts documented for numerous plant species (Chen et al., 2011; Lenoir et al., 2008). In contrast, precipitation-related variables—particularly BIO8 and BIO19—exhibited notable declining contributions over the four decades, reflecting the fact that date palm is inherently adapted to arid conditions with minimal rainfall requirements during the growing season (Morton, 1987).

The spatial patterns of climatic suitability change revealed a consistent west-to-east shift in suitable habitats over the four-decade study period, with decreased suitability concentrated in western and southwestern provinces (Khuzestan, Fars, Bushehr) and increased suitability primarily observed in southeastern and eastern provinces (Kerman, Sistan and Baluchestan, South Khorasan). This directional shift is consistent with projected expansions of suitable regions in central and eastern Iran under future climate scenarios (Shabani et al., 2013; Baaghideh et al., 2020), providing empirical evidence that this shift is already underway.

The binary classification analysis revealed that unsuitable areas expanded consistently from 74.24% to 74.71% of Iran's total land area, suggesting a net contraction of climatically suitable regions despite localized improvements. Elevation remained a consistent constraint, with suitability declining rapidly above 500 m a.s.l., indicating limited scope for upward range shifts and underscoring the importance of considering topographic constraints alongside climatic variables. The findings have important implications for date palm cultivation and climate adaptation planning: expansion should be prioritized in southeastern provinces where conditions are becoming increasingly favorable, while continued investment in western and southwestern provinces may face increasing climate-related risks, including heat stress and the bunch drying disorder (Najafiniya and Rahkhodaei, 2024).

The increasing importance of temperature highlights the need for heat-tolerant cultivars, with breeding programs prioritizing traits associated with heat and drought tolerance. This retrospective analysis provides a valuable benchmark against which future projections can be validated, supporting

previous studies that projected substantial increases in suitable areas in central and eastern Iran (Shabani et al., 2013; Afzali et al., 2022). However, the results also highlight the importance of considering extreme climatic events alongside mean parameters, as the bunch drying disorder—triggered by temperatures exceeding 43°C combined with low humidity—represents a critical threat not captured by mean variables alone. Future research should integrate higher-resolution climate data, incorporate soil and water variables, validate predictions against independent data, and assess the economic implications of suitability shifts.

5. Conclusion

This study provides the first retrospective, multi-decadal assessment of climatic suitability shifts for date palm in Iran, filling a critical gap between future projections and historical observations. The results demonstrate that:

- Temperature is the primary driver of date palm distribution, with BIO1 (Annual Mean Temperature) accounting for 68.1% of model contribution across all decades. The thermal optimum has shifted upward by approximately 1°C from the 1980s to the 2010s.
- A consistent west-to-east shift in suitable habitats has occurred over the four-decade study period, with decreased suitability in western and southwestern provinces (Khuzestan, Fars, Bushehr) and increased suitability in southeastern and eastern provinces (Kerman, Sistan and Baluchestan, South Khorasan).
- Unsuitable areas have expanded from 74.24% to 74.71% of Iran's total land area, suggesting a net contraction of climatically suitable regions despite localized improvements.
- Elevation remains a consistent constraint, with suitability declining rapidly above 500 m a.s.l., indicating limited scope for upward range shifts.
- Extreme climatic events—particularly temperatures exceeding 43°C combined with low humidity—pose a significant threat that is not captured by mean climatic variables alone and warrants explicit incorporation into future suitability assessments.

These findings provide a scientific basis for climate adaptation planning in Iran's date palm sector, including strategic orchard relocation, cultivar selection, and irrigation management.

Contributions

Zahra Hosseini: Conceptualization, Methodology, Investigation, Formal analysis, Resources, Software, Writing - Review & Editing. **Javad Bazrafshan and Arezoo Nazi Ghameshlou**: Conceptualization, Investigation, Supervision, Writing - Review & Editing.

Ethics declarations

Conflict of interest

The authors declare no competing interests.

Funding Declaration

The authors declare no funding.

References

Afzali, S., Khoshhal Dastjerdi, J. and Torahi, A. (2022). Predicting Changes in Cultivation of Gantar and Halawi Dates in Iran in the 21st Century. *Water and Soil*, 35(6), 902-922.

Alizadeh-Choobari, O., and Najafi, M. S. (2018). Extreme weather events in Iran under a changing climate. *Climate Dynamics,* 50, 249-260.

Allbed, A., Kumar, L., and Shabani, F. (2017). Climate change impacts on date palm cultivation in Saudi Arabia. *The Journal of Agricultural Science*, 155(8):1203-1218.

Anshida, M., Murugan, P. P., Senthilkumar, M., Chandrakumar, M., Vanitha, G., Rani, A. J., and Arvind, G. (2026). Impact of climate change on food security: A systematic literature review and bibliometric analysis. *Sustainable Futures*, 11, 101826.

Araújo, M.B., Whittaker, R.J., Ladle, R.J., and Erhard, M. (2005). Reducing uncertainty in projections of extinction risk from climate change. *Global Ecology and Biogeography*, 14(6), 529–538.

Asadi-RahimBeygi, N., Mofidi, A., Zarrin, A., and Dadashi-Roudbari, A. (2025). Near-term climate extremes in Iran based on compound hazards analysis. *Scientific Reports*, 15, 43843.

Baaghideh, M., Azizzadeh, J., Ahmadi, H., and Entezari, A. (2020). Climate change impacts on the cultivation areas of date palm tree in Iran. *Arabian Journal of Geosciences*, 13, 1188.

Bazrafshan, J. (2017). Effect of air temperature on historical trend of long-term droughts in different climates of Iran. *Water Resources Management*, 31, 4683-4698.

Bazrafshan, J., Hejabi, S., and Eslamian, S. (2017). Drought Modeling Examples. In: "Handbook of Drought and Water Scarcity" (E. S. and E. F., eds.), Vol. 1: Principles of Drought and Water Scarcity, pp. 167-188. Francis and Taylor, CRC Press, USA.

Booth, T.H. (2018). Species distribution modelling tools and databases to assist managing forests under climate change. *Forest Ecology and Management*, 430, 196–206.

Booth, T.H., Nix, H.A., Busby, J.R., and Hutchinson, M.F. (2014). BIOCLIM: The first species distribution modelling package, its early applications and relevance to most current MaxEnt studies. *Diversity and Distributions*, 20(1), 1–9.

Challinor, A. J., Parkes, B., and Ramirez-Villegas, J. (2015). Crop yield response to climate change varies with cropping intensity. *Global Change Biology*, 21(4), 1679-1688.

607 Chao, C.T., and Krueger, R.R. (2007). The date palm (*Phoenix dactylifera* L.): Overview of biology, uses,
608 and cultivation. *HortScience*, 42(5), 1077–1082.
609 Chen, I.C., Hill, J.K., Ohlemüller, R., Roy, D.B., and Thomas, C.D. (2011). Rapid range shifts of species
610 associated with high levels of climate warming. *Science*, 333(6045), 1024–1026.
611 Dawson, T. P., Jackson, S. T., House, J. I., Prentice, I. C., and Mace, G. M. (2011). Beyond predictions:
612 Biodiversity conservation in a changing climate. *Science*, 332(6025), 53–58.
613 Dobrowski, S.Z., Thorne, J.H., Greenberg, J.A., Safford, H.D., Mynsberge, A.R., Crimmins, S.M., and
614 Swanson, A.K. (2011). Modeling plant ranges over 75 years of climate change in California, USA:
615 Temporal transferability and species traits. *Ecological Monographs*, 81(2), 241–257.
616 Dudik, M., Phillips, S.J., Schapire, R.E., Dud, M., and Schapire, R.E. (2007). Maximum Entropy
617 Density Estimation with Generalized Regularization and an Application to Species Distribution
618 Modeling. *Journal of Machine Learning Research*, 8, 1217–1260.
619 Elith, J., Phillips, S.J., Hastie, T., Dudík, M., Chee, Y.E., and Yates, C.J. (2011). A statistical explanation
620 of MaxEnt for ecologists. *Diversity and Distributions*, 17(1), 43–57.
621 Fahad, S., Bajwa, A. A., Nazir, U., Anjum, S. A., Farooq, A., Zohaib, A., Sadia, S., Nasim, W., Adkins,
622 S., Saud, S., Ihsan, M. Z., Alharby, H., Wu, C., Wang, D., and Huang, J. (2017). Crop production
623 under drought and heat stress: plant responses and management options. *Frontiers in Plant Science*,
624 8, 1147.
625 FAO (2026). FAOSTAT: Crops and livestock products [Internet]. Rome: FAO. [Available
626 from: https://www.fao.org/faostat/en/#data/QCL]
627 Feng, X., Park, D. S., Liang, Y., Pandey, R., and Papeş, M. (2019). Collinearity in ecological niche
628 modeling: Confusions and challenges. *Ecology and Evolution,* 9, 10365-10376.
629 Fick, S.E., and Hijmans, R.J. (2017). WorldClim 2: New 1 km spatial resolution climate surfaces for
630 global land areas. *International Journal of Climatology*, 37(12), 4302–4315.
631 Guisan, A., Tingley, R., Baumgartner, J. B., Naujokaitis-Lewis, I., Sutcliffe, P. R., Tulloch, A. I., Regan,
632 T. J., Brotons, L., McDonald-Madden, E., and Mantyka-Pringle, C. (2013). Predicting species
633 distributions for conservation decisions. *Ecology letters*, 16, 1424-1435.
634 Heikonen, S., Heino, M., Jalava, M., Siebert, S., Viviroli, D., and Kummu, M. (2025). Climate change
635 threatens crop diversity at low latitudes. *Nature Food,* 6, 331-342.
636 Hultgren, A., Carleton, T., Delgado, M., Gergel, D. R., Greenstone, M., Houser, T., Hsiang, S., Jina,
637 A., Kopp, R. E., Malevich, S. B., McCusker, K. E., Mayer, T., Nath, I., Rising, J., Rode, A., and
638 Yuan, J. (2025). Impacts of climate change on global agriculture accounting for adaptation. Nature
639 642, 644-652.

Hussain, M., Ismailli, N.J., and Jiskani, A.M. (2020). Effect of humidity on growth and development of fungal pathogens of ripening dates (*Phoenix dactylifera* L.) at Khairpur, Pakistan. *Plant Protection*, 4(1), 11–16.

Ismail, M.H., Ali, S.A., and Abd, G.I. (2023). The seasonal fluctuations in weather and their impact on the flowering, fruit setting, and growth of date palm fruits (*Phoenix dactylifera* L.) in Iraq. *Samarra Journal of Pure and Applied Science*, 5(2).

Jahanshahi, A., Booij, M. J., Patil, S. D., and Gupta, H. (2024). An ensemble-based projection of future hydro-climatic extremes in Iran. *Journal of Hydrology*, 642, 131892.

Jamali, M., Eslamian, S., Shayannejad, M., and Gohari, A. (2026). Observed warming–driven aridification and climate-type transitions across Iran. *Journal of Arid Environments,* 235, 105606.

Karger, D. N., Conrad, O., Böhner, J., Kawohl, T., Kreft, H., Soria-Auza, R. W., Zimmermann, N. E., Linder, H. P., and Kessler, M. (2017). Climatologies at high resolution for the earth's land surface areas. *Scientific Data* **4**, 170122.

Khalili, A., and Rahimi, J. (2018). Climate. In "The Soils of Iran" (M. H. Roozitalab, H. Siadat and A. Farshad, eds.), pp. 19-33. Springer International Publishing, Cham.

Lenoir, J., Gégout, J.C., Marquet, P.A., de Ruffray, P., and Brisse, H. (2008). A significant upward shift in plant species optimum elevation during the 20th century. *Science*, 320(5884), 1768–1771.

Marzban, C. (2004). The ROC Curve and the Area under It as Performance Measures. *Weather and Forecasting* **19**, 1106-1114.

Merkenschlager, C., Bangelesa, F., Paeth, H., and Hertig, E. (2023). Blessing and curse of bioclimatic variables: A comparison of different calculation schemes and datasets for species distribution modeling within the extended Mediterranean area. Ecology and Evolution, 13, e10553.

Mihi, A., and Hernández-Agüero, J.A. (2025). Saharan date palm plantation doubled in Algeria over the last four decades insofar as northern plantation expanded. *Computers and Electronics in Agriculture,* 237, 110649.

Mihi, A., Tarai, N., and Chenchouni, H. (2019). Can palm date plantations and oasification be used as a proxy to fight sustainably against desertification and sand encroachment in hot drylands? *Ecological Indicators,* 105, 365-375.

Modarres, R., and Sarhadi, A. (2009). Rainfall trends analysis of Iran in the last half of the twentieth century. *Journal of Geophysical Research: Atmospheres*, 114, D03101.

Morton, J.F., 1987. Fruits of warm climates. Creative Resource Systems Inc., Winterville, N.C., USA.

Najafiniya, M., and Rahkhodaei, E. (2024). A review on date palm (Phoenix dactylifera) fruit bunch wilting disorder in Iran. *Indian Phytopathology,* 77, 271-281.

673 Nemati, Z., Zeinalabedini, M., Majidian, P., Jahromi, A.E., and Kiani, D. (2014). Phylogenetic
674 relationships among Iranian and Spanish date palms (*Phoenix dactylifera* L.) revealed by
675 microsatellite markers. *Journal of Horticultural Science and Biotechnology*, 89(2), 114–120.
676 Phillips, S.J., Anderson, R.P., and Schapire, R.E. (2006). Maximum entropy modeling of species
677 geographic distributions. *Ecological Modelling*, 190(3–4), 231–259.
678 Phillips, S.J., Anderson, R.P., Dudík, M., Schapire, R.E., and Blair, M.E. (2017). Opening the black
679 box: An open-source release of Maxent. *Ecography*, 40(7), 887–893.
680 Proctor, J., Zeppetello, L. V., Chan, D., and Huybers, P. (2025). Climate change increases the
681 interannual variance of summer crop yields globally through changes in temperature and water
682 supply. *Science Advances,* 11, eady3575.
683 Ramirez-Cabral, N.Y.Z., Kumar, L., and Shabani, F. (2017). Global alterations in areas of suitability
684 for maize production from climate change and the use of agricultural management
685 scenarios. *Global Change Biology*, 23(9), 3810–3825.
686 Shabani, F., and Kumar, L. (2014). Sensitivity analysis of CLIMEX parameters in modeling potential
687 distribution of *Phoenix dactylifera* L. *PLoS ONE*, 9(4), e94867.
688 Shabani, F., Kumar, L., and Ahmadi, M. (2017). Variances in the projections, resulting from CLIMEX,
689 Boosted Regression Trees and Random Forests techniques. *Theoretical and Applied Climatology*, 129,
690 801–814.
691 Shabani, F., Kumar, L., and Solhjouy-Fard, S. (2013). Impacts of climate change on date palm
692 distribution in Iran using CLIMEX. *Journal of Agricultural Science and Technology*, 15, 1019–1030.
693 Shabani, F., Kumar, L., and Taylor, S. (2012). Climate change impacts on the future distribution of
694 date palms: A modeling exercise using CLIMEX. *PLoS ONE*, 7(10), e48021.
695 Swets, J.A. (1988). Measuring the accuracy of diagnostic systems. Science (New York, N.Y.), 240(4857),
696 1285–1293.
697 Tabari, H., and Talaee, P.H. (2011). Analysis of trends in temperature data in arid and semi-arid regions
698 of Iran. *Atmospheric Research*, 101(1–2), 1–11.
699 Tuninetti, M., and Davis, K.F. (2026). Addressing global hotspots of drought-related crop production
700 losses. Nature Communication, 17, 6605
701 Wang, Y., Ren, X., Wang, K., Lin, W., Wang, P., Liu, Z., Zhang, H., and Zhou, N. (2025). Maxent
702 model-based prediction of the potential distribution of Fritillaria taipaiensis P. Y. Li. *Scientific*
703 *Reports*, 15, 20837.
704 Warren, D.L. and Seifert, S.N. (2011), Ecological niche modeling in Maxent: the importance of model
705 complexity and the performance of model selection criteria. Ecological Applications, 21: 335-342.

706 Watling, J.I., Brandt, L.A., Bucklin, D.N., Fujisaki, I., Mazzotti, F.J., Romañach, S.S., and Speroterra,
707 C. (2021). Performance metrics and variance partitioning reveal sources of uncertainty in species
708 distribution models. *Ecological Modelling*, 452, 109570.
709 Yackulic, C.B., Chandler, R., Zipkin, E.F., Royle, J.A., Nichols, J.D., Campbell Grant, E.H., and Veran,
710 S. (2013). Presence-only modelling using MaxEnt: When can we trust the inferences? *Methods in*
711 *Ecology and Evolution*, 4(3), 236–243.
712 Zaid, A., and de Wet, P.F. (2002). *Climatic Requirements of Date Palm*. In: Date Palm Cultivation (Zaid,
713 A., ed.), Second edition. FAO Plant Production and Protection Paper Series, No. 156. Rome:
714 FAO.
715
716
717
718
719